

## EXPERIMENTAL INVESTIGATION OF AN UNSTEADY FLOW FIELD AROUND AN AIRFOIL

*A. Hribernik, M. Fike, G. Bombek, M. Hribersek*

Faculty of Mechanical Engineering, University of Maribor, Slovenia, [ales.hribernik@uni-mb.si](mailto:ales.hribernik@uni-mb.si)

**Abstract:** A small wind tunnel where basic aerodynamic properties such as the lift, drag, and pressure distribution of an airfoil can be measured was used to study an unsteady flow-field around an isolated airfoil. Transparent walls enabled the application of PIV (Particle Image Velocimetry) so as to acquire a 2D velocity-field around the considered airfoil. A study was performed at various angles of attack (AOA). No separation was observed at low AOA. At 10 °AOA, the separation vortex comprised 50 % of the airfoil's chord-length, whilst complete stalling of the airfoil occurred at 20 °AOA. The observed separation zone was not fixed but was found to oscillate around its mean-position at an interval of  $\pm 10$  % of the chord's length.

**Keywords:** airfoil, flow separation, PIV measurement.

### 1. INTRODUCTION

An axial fan may be treated as an incompressible turbomachine device, producing large gas-flow rates and small pressure rises. However, during many applications such as cooling and ventilating systems, axial fans have to operate within limited space conditions and have to provide higher pressure rises at lower flow-rates, than they are designed for. The operation of an axial fan in conditions of increasing back-pressure causes flow-separation at the suction sides of fan blades and eventually leads to blade-stalling, which results in unsteady fan-operation characterized by heavy variations of flow-rate and pressure rise. The prediction of axial fan operation under design conditions can be very successful by using CFD simulations, whilst, on the other hand, only poor agreement is achieved of stalling axial-fan's simulations with experimental results. One of the reasons is the complexity of such simulations and the lack of an appropriate model for correctly predicting flow-separation. The latter can be effectively studied on an isolated airfoil, by increasing the angle of attack leading to flow-separation, similar to that on the fan's blade by reduced flow and an increased incidence angle.

Few studies have been carried out to investigate the unsteady properties of flow-separation on an airfoil at moderate Reynolds numbers which correspond to a fan-operating condition near or on the stall line, at a very low flow rate [1]. The interest of research into unsteady flow around airfoils comes from the appearance of unsteadiness despite steady freestream conditions. It leads to great unsteadiness of the local flow properties such as the

boundary layer behaviour, and in global parameters such as aerodynamical loads [2]. Unsteadiness is the reason for significant oscillations in local flow characteristics such as boundary layer changes and integral characteristics such as drag and lift coefficients. It was reported that the position of the separation point in the case of turbulent boundary layer is static [3]. Furthermore, Nishimura and Taniike [4] showed a correlation between the separation point location and the lift coefficient, and a connection between the frequency of position change and von Karman's instability.

The purpose of the work presented here is firstly to characterize the aerodynamics of a fan airfoil experimentally, so that the results obtained constitute a two-dimensional experimental results database to be used in three-dimensional fan simulations, using the commercial CFD code. Moreover, the data can be analysed to exhibit the mechanisms responsible for flow-separation and its influence on lift and drag. The airfoil studied was S 809 and is widely used due to a convenient lift/drag coefficient.

### 2. METHODOLOGY

#### 2.1. Wind tunnel

The experimental measurements were conducted within a small wind tunnel. The air to the test rig was supplied by a radial fan driven by a 15 kW electrical motor, the rotational speed of which was controlled by a variable frequency drive. The air entered the settling chamber via a conical entrance section at an angle of 30°. The cross-section of the settling chamber was 1100 x 1100 mm. The settling chamber was equipped with a combination of perforated plates, honeycombs, and meshes in order to reduce unsteadiness and any swirl in the flow. The air was then accelerated by a converging nozzle into a rectangular test section measuring 200 mm (height) by 200 mm (width). The air exiting the test-section was vented into the atmosphere. The maximum air velocity in the tunnel was 50 m/s and turbulent intensity, measured by hot-wire anemometry was 1.5 %. A single fan blade with a S 809 profile and a chord length ( $c$ ) of 100 mm was centrally mounted within the test-section. The span of the airfoil was 200 mm and the median section was equipped with pressure taps at the positions indicated in Fig. 1. The airfoil was produced using rapid prototyping which allowed holes for the pressure taps to be created during the production process with no unnecessary extra drilling. 16 positions for pressure measurements were applied. 50 mm-long pneumatic tubes were used for

connecting with the sensors. The sinusoidal response of the plastic tubing and sensors was, therefore, satisfactory for frequencies of up to 300 Hz, since the gain factor was less than 1.05 [5]. The frequency response of the system was, therefore, satisfactory because the phenomena investigated, in particular Von Karman vortex shedding, had a characteristic frequency below 300 Hz. Pressure sensors GMSD 2.5 MR and GMSD 25 MR were used, with different measurement uncertainties of 0.5 Pa and 5 Pa, respectively. Pressure signals within duration of 10 seconds were acquired with 1 kHz sampling frequency.

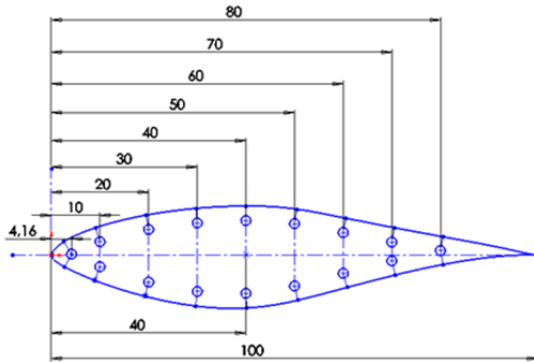


Fig. 1. Geometry of airfoil and pressure taps' locations

A transparent extension was added to the wind-tunnel to enable PIV measurements (Fig. 2). The extension and the airfoil fixture enabled a setting of airfoil's angle of attack.

### 2.1. PIV system

PIV (Particle Image Velocimetry) was used to capture the flow field around the airfoil. Camera and laser were placed on a lightweight traverse system originally used for LDA measurements. A measurement plane was placed in the middle of the airfoil to reduce the influence of the wall (Fig. 2). A two-cavities Nd: YAG laser was used, operating at high-power with 50 mJ pulse energy. The frequency of bursts was 4 Hz. For the PIV experiments, 1-3  $\mu\text{m}$  oil droplets generated by a Polytec L2F-A-1000 Aerosol Generator were injected upstream of the settling-chamber. This guaranteed a homogeneous seeding density within the test-section. The laser was placed downstream at approximately 1 m from the airfoil. A CCD camera with 1280x1024 pixels resolution was used and the area covered was approx. 120 x 100 mm. The time-interval between the laser pulses was 20  $\mu\text{s}$ . 32x32 pixels size interrogation areas were used for velocity calculation. Cross-correlation and adaptive correlation were used, both with 25% overlap.

Several parameters have to be considered for estimating the uncertainties of the PIV velocity measurements [6]. Systematic errors occur due to uncertainties when determining the geometrical parameters and the fabrication tolerances of the camera devices and lenses. Non-systematic errors are mainly due to the uncertainty when determining the average particle displacement within the interrogation region. As the flow in the test-section was quasi two-dimensional, the out-of-plane component of the vectors only caused negligible errors. Lehr and Boelcs [7] showed that

for these conditions the standard measurement uncertainty for the mean velocity field is less than  $0.04 u_\infty$ , in regions of strong velocity gradients it is smaller than  $0.05 u_\infty$ .

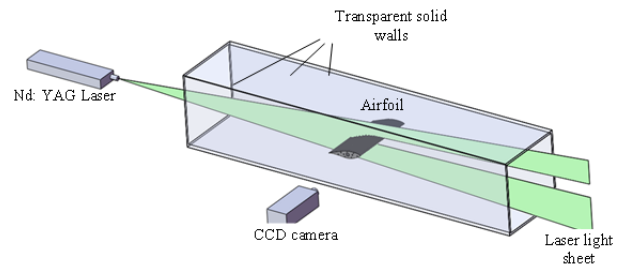


Fig. 2. The PIV measurement system

## 3. RESULTS AND DISCUSSION

The measurements were performed at  $Re = 2 \times 10^5$  and different AOA's of  $0.7^\circ$ ,  $5.1^\circ$ ,  $9.6^\circ$ ,  $15.1^\circ$ , and  $20.0^\circ$ , respectively. When the angle of attack was increased a complex stall-phenomenon occurred on the suction-side of the airfoil. This was caused by flow-separation and an adverse pressure-gradient. Simpson et al. [3] reported that the position of flow-separation in the case of a turbulent boundary layer oscillates and they proposed a set of quantitative definitions on the detachment state near the wall using definitions based on the fraction of time the flow moves downstream. Four characteristic points were defined: incipient detachment (ID) occurred with an instantaneous backflow 1% of the time, transitory detachment (TD) occurred with an instantaneous backflow 50% of the time, and detachment (D) occurred where the time-averaged wall shearing stress was equal to zero. Available data indicated that points TD and D were at the same location [3]. Finally, the characteristic point  $D_{cp}$  determines a critical position downstream of which the flow is detached at any time. Different experimental methods or CFD simulation can be applied to obtain characteristic points of flow-separation.

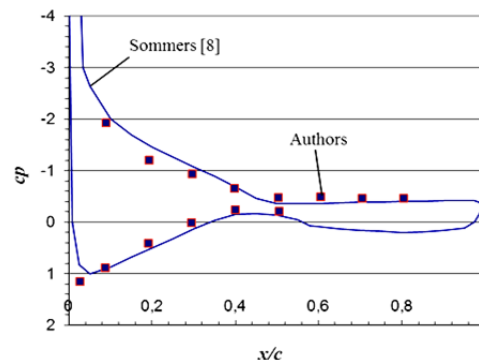


Fig. 3. Pressure coefficient profile for  $AOA = 15.1^\circ$

Table 1. Comparison between the experimentally-obtained positions ( $x/c$ ) of the characteristic points (ID, TD, Dcp) of the flow separation zone

	Angle of attack ( $^\circ$ )										
	0.7	5.1	9.6			15.1			20		
			ID	TD	Dcp	ID	TD	Dcp	ID	TD	Dcp
Pressure signal analysis	NS*	NS	0.45		0.65	0.30		0.55	0.00		0.20
PIV images analysis	NS	NS	0.48	0.52	0.66	0.40	0.47	0.62	0.02	0.04	0.11

\*NS – no separation occurred

### 3.1. Validation

The present measurements were validated by comparing current data in the steady case, with those obtained by Sommers et al. [8]. Fig. 3 shows the comparison of pressure coefficient profile at AOA = 15.1  $^\circ$ . The pressure is given in the usual form of pressure coefficient:

$$c_p = \frac{p - p_\infty}{\frac{1}{2} \rho u_\infty^2} \quad (1)$$

where  $p_\infty$  is the freestream static pressure and  $u_\infty$  is the freestream velocity far upstream from the airfoil. The measurement uncertainty of pressure coefficient at each measurement point was less than 0.5 %. The agreement was good (Fig. 3) and ensured that the present measurements, in the steady case, are correct.

### 3.2. Pressure tap signals analysis

According to Sicot et al. [2] the oscillation zone of the flow-separation point can be obtained using statistical analysis of signals from pressure taps along the suction side of the airfoil by relating the increase in measurement dispersion to the oscillation of the flow separation point position and the separation area. Standard deviation can be used as a measure of measurement dispersion. Therefore, suction-side pressure tap signals were statistically analysed, their standard deviations were normalised and compared (Fig. 4). The curve connecting these values for specific AOA (curve for AOA = 9.6  $^\circ$  as shown in Fig. 4) had two characteristic points. The first one corresponded to incipient detachment point (ID). The ID point represented the position of the separation point where alternations between attached and separated flow occurred. Therefore, the pressure fluctuations at the ID point were the greatest, thus it coincided with the local maximum value of normalized standard deviation. Upstream of ID the flow was attached at any moment. The characteristic point – Dcp, downstream of which the flow is at any time detached, corresponds according to Sicot et al. [2], to the local minimum of standard deviation. The interval between the ID and Dcp points locates the oscillation zone of the separation point and can be estimated by analyzing the standard deviation of the signal from different pressure taps. The error made using this method comes from the discontinuous distribution of the pressure taps. The resolution was quite low in our case

since only 8 pressure taps were applied on the airfoil suction surface.

As presented in Fig. 4, the pressure oscillations along the airfoil suction-side differed from position to position and were angle of attack dependent (see also Table 1). The separation point ID (local standard deviation maximum) moved towards the leading-edge when AOA increased and vice versa. In the case of 20  $^\circ$  AOA, permanent flow-separation occurred at or before  $x/c = 0.2$  (local standard deviation minimum). Separation temporarily occurred at or before  $x/c = 0.1$  (local standard deviation maximum) thus the oscillation zone of flow-separation point was located at between  $0.0 < x/c < 0.2$ . In the cases of 15.1  $^\circ$  AOA and 9.6  $^\circ$  AOA, oscillation zones were found between  $0.25 < x/c < 0.55$  and  $0.45 < x/c < 0.65$ , respectively, whilst no separation could be proven in the cases of 5.1  $^\circ$  AOA and 0.7  $^\circ$  AOA. Similar results may be obtained from measured velocity fields acquired by the PIV method, which will be presented next.

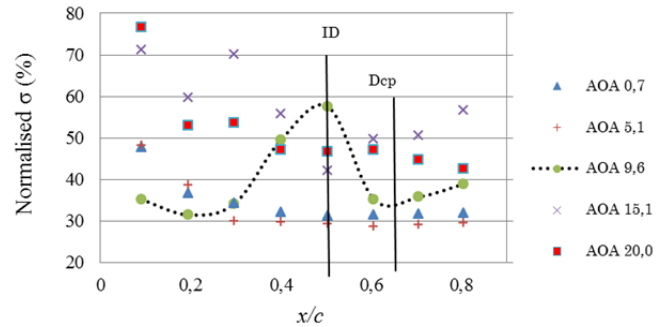


Fig. 4. Variation of normalised standard deviation of pressure signals from successive pressure taps on the suction side of the airfoil

### 3.3. PIV images analysis

The PIV system applied during our research operated at frequencies of up to 4 Hz and disallowed direct time-dependent analysis of the flow-field around the airfoil. Thus, at least 60 consecutive images were acquired and their corresponding velocity fields established. In the first step, the velocity field was averaged in order to find the main velocity field pattern as one presented in Fig. 5a. This was then used to compute vorticity field (Fig. 5b). The obtained average vorticity field shows the formation of two shear

layers, one from the leading edge and one from the trailing edge. The formation length was greater from the leading edge ( $l_2$ ) than from the trailing edge ( $l_1$ ). A sudden growth of the average shear layer, combined with a roll-up of the shear layer, was observed downstream of the airfoil. Similar results were obtained by Sicot et al. [2] and Yang et al. [9] when both investigated the flow-field around an isolated airfoil at moderate Re numbers.

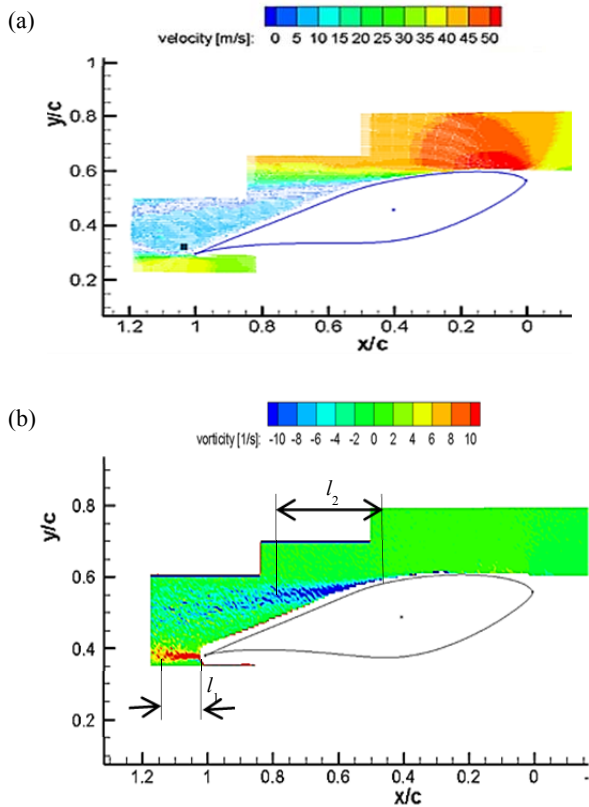


Fig. 5. Averaged velocity (a) and corresponding vorticity (b) field  $AOA = 15.1^\circ$

The fluctuating nature of the flow-separation which was discussed in the section 3.2 was quite evident from PIV images. Two characteristic images that proved the oscillation of the flow-separation point are presented in Fig. 6. Whilst in the bottom image flow separation occurred at  $x/c = 0.4$ , it shifted towards the trailing-edge of the airfoil to  $x/c = 0.6$  in top image. Both values can be found within the separation-zone interval obtained from the pressure signals (see Table 1).

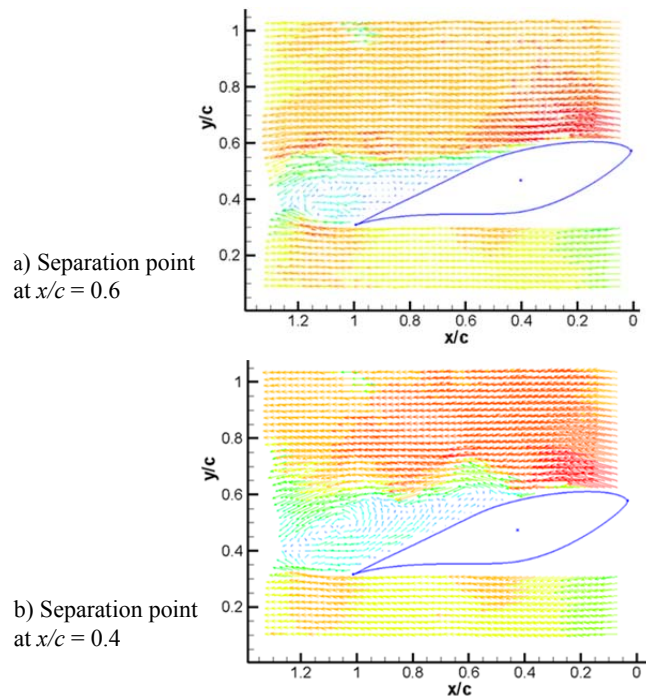


Fig. 6. Two characteristic PIV images proving the oscillation of the flow-separation point  $AOA = 15.1^\circ$

By careful analysis of a series of PIV images taken at the same position over a longer period of time, the separation zone could be further studied in order to predict not only both extreme points ID and Dcp, but also to estimate the percentage of back flow in any point within the separation zone. A program was developed in LabVIEW to use the PIV results and extract all the values for each vector (velocity components, position, and status). It was possible to analyse the data and calculate the medium value and standard deviation for velocity and its direction (angle). It was also possible to count those cases where the angle differed from the chord angle by more than a certain value. If the value was set at  $90^\circ$  the result represented backflow occurrence. This value could be divided by the number of images resulting in a backflow occurrence ratio. The results could be presented as intensity graphs, as shown in Figure 7. As can be seen from Fig. 7b ( $AOA = 15.1^\circ$ ) the alternations between the attached and separated flows (ID point) occurred at  $x/c = 0.4$  (area with 0 to 10 % of backflow). At  $x/c = 0.47$  the flow was reversed 50 % of the time, thus this point corresponded to the transitory detachment (TD) point, at  $x/c = 0.62$  the flow was detached at any time and corresponded to the Dcp point. Similarly, the series of images at all other AOA were analysed and the results are presented in Table 1 for comparison with the pressure signal-based method.

## 5. REFERENCES

- [1] Moreau, S., Christophe, J., Roger, M., LES of the trailing-edge flow and noise of a NACA0012 airfoil near stall. *Proceedings of the Summer Program 2008*, Center for Turbulence Research, Stanford Univ./NASA Ames.
- [2] Sicot, C., Aubrun, S., Loyer, S., Devinan, P., Unsteady characteristics of the static stall of an airfoil subjected to freestream turbulence level up to 16%. *Experiments in Fluids*, **41** 641–648. (2006)
- [3] Simpson, R.L., Chew, Y.T., Shivaprasad, B.G., The structure of a separating turbulent boundary layer: part I, mean flow and Reynolds stresses; part II, higher order turbulence results. *The Journal of Fluid Mechanics* **113**, 23–73. (1981)
- [4] Nishimura, H., Taniike, Y., Aerodynamics characteristics of fluctuating forces on a circular cylinder. *Journal of Wind Engineering and Industrial Aerodynamics*, **89(7)** 713–723. (2001)
- [5] Chapin, W. G., Dynamic-pressure measurement using an electronically scanned pressure module, NACA TM-84650, (1983)
- [6] Raffel, M., Willert, C., Kompenhans, J., Particle Image Velocimetry, A Practical Guide, ISBN 3-540-63683-8, Springer-Verlag 1998
- [7] Lehr A., Böls A., 2000: Application of a Particle Image Velocimetry System to the Investigation of Unsteady Transonic Flows in Turbomachinery, *9th International Symposium on Unsteady Aerodynamics, Aeroacoustics and Aeroelasticity of Turbomachines*, Lyon, 4-8 September, 2000
- [8] Sommers, D.M. Design and Experimental Results for the S809 Airfoil. NREL/SR-440-6918, (1997)
- [9] Yang, Z., Haan, F. L., Hui, H., Ma, H. (2007). An Experimental Investigation on the Flow Separation on a Low-Reynolds-Number Airfoil, *45th AIAA Aerospace Sciences Meeting and Exhibition*, Reno Nevada, USA, AIAA-2007-0275.

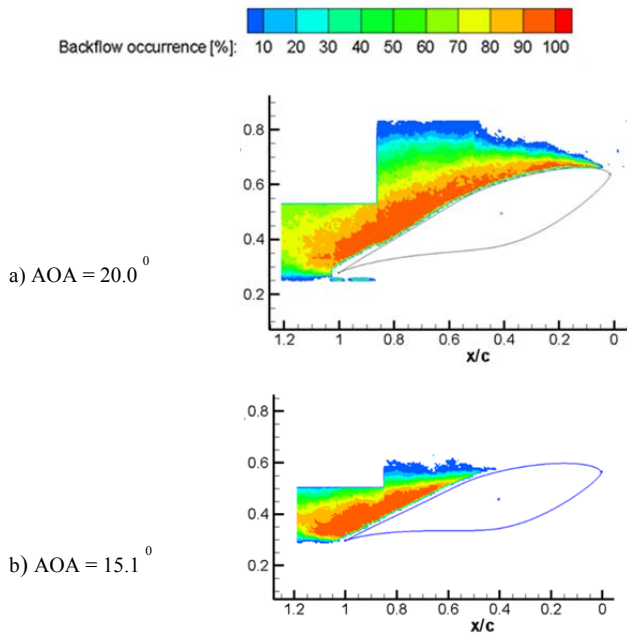


Fig. 7. Intensity graph of backflow occurrence ratio

## 4. CONCLUSIONS

The presented study investigated the unsteady properties of the separation zone on a two-dimensional airfoil. In particular, the oscillation of the separation point was studied in two ways. A local approach was used to study the oscillation of the separation point on the suction surface of the airfoil, through simultaneous surface pressure measurements around the airfoil. A method was used for determining the length of the separation point oscillation zone from the standard deviation of pressure-signals. It showed that the length of the oscillation zone increased when the separation point moved towards the leading edge. PIV measurements were performed in order to obtain a global insight of the instantaneous flow field around the airfoil, and to check whether the length of the oscillation zone was correctly determined. A program was developed in LabVIEW to use the PIV results and to predict the backflow occurrence ratio along the airfoil, which was then used to locate the position of the separation-point's oscillation zone. Both approaches showed similar results which confirmed the pressure signal-based approach proposed by Sicot [2]. In future work, the mechanisms of separation-point oscillation on a partially separated airfoil, such as coupling with von Karman vortex shedding, needs to be investigated in greater depth through additional high-rate PIV and LDA measurements.